American Journal of Energy Engineering
2025, Vol. 13, No. 3, pp. 150-157
https://doi.org/10.11648/j.ajee.20251303.16

Research Article

Dynamic Frequency Study Under Monochromatic Illumination of the Photocurrent Density - Photovoltage Characteristic and the Series and Shunt Resistances of a Solar Cell Based on CIGS: Effects of the Angle of Incidence and the Doping Level of Gallium

Gerome Sambou*, Ibrahima Wade, Khamissa Diallo, Djimba Niane, Moustapha Dieng

Physics Department, University Cheikh Anta Diop, Dakar, Senegal

Abstract

This article focuses on the analysis of a CIGS (copper, indium, gallium, selenide) solar cell using a dynamic frequency approach under monochromatic illumination. The main objective is to understand the behavior of the cell and identify the factors that influence its performance, particularly the angle of incidence of light and the gallium doping rate. The work begins with solving the differential equation that governs the dynamics of minority charge carriers within the cell. This solution provides an analytical expression for the density of these carriers, which is a crucial step in modeling the electrical behavior of the cell. From this carrier density, expressions for the photocurrent density and photovoltage are then derived. The study of the photocurrent-photovoltage characteristic, often referred to as the I-V (current-voltage) curve, is central to the analysis. This curve reveals two key operating points for the solar cell. The first is short-circuit operation, where the photocurrent reaches its maximum value and remains relatively constant. The second is open-circuit operation, characterized by very low photocurrent values, where the voltage is at its maximum. The results of the study show a correlation between the angle of incidence of light and the performance of the cell. An increase in the angle of incidence leads to a significant decrease in the photocurrent module. This is logical, as a more oblique incidence reduces the amount of light absorbed by the cell. The study also reveals that the open-circuit operating point decreases slightly as the angle of incidence increases. In contrast, the gallium doping level has a more pronounced impact on the open-circuit operating point, suggesting a deeper influence on the internal properties of the material. Finally, the article uses electrical models to deduce the values of the cell's series and shunt resistances, based on the observed operating points. This analysis shows that both the angle of incidence and the gallium doping rate tend to increase these resistances. These increases can degrade cell performance by introducing energy losses, highlighting the importance of these two parameters in the design and optimization of CIGS solar cells.

Keywords

CIGS, Frequency Modulation, Wavelength, Incidence Angle, Gallium Doping Rate, Serie Resistance, Shunt Resistance

*Corresponding author: sambougerome@yahoo.fr (Gerome Sambou)

Received: 2 August 2025; **Accepted:** 14 August 2025; **Published:** 15 September 2025

1. Introduction

The success of thin CIGS film modules is based on their low production cost and relative high efficiency [1].

Nevertheless, the modules are affected by defects occurring in the production processes or later during operation in the field. One prominent representative of those device defects is an ohmic shunt, and s érie who limitide the solar cell performance [2].

The simulation study allows linking the cell parameters with its performance. In this work, a study in dynamic frequency regime has been conducted on a CIGS-based solar cell. The resolution of the differential equation describing the behavior of minority carriers made it possible to determine the density of minority carriers. From this density, the photocurrent density and the photovoltage will be deduced. In this article, we study the photocurrent density -photovoltage characteristic and the shunt and series resistances under the effect of the angle of incidence of the incident ray and the doping level with Gallium.

2. Theoretical Study

We consider a CIGS-based solar cells whose simplified structure is shown in Figure 1.

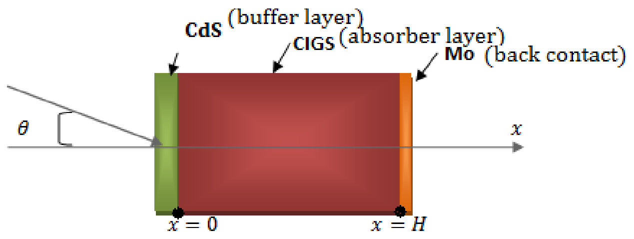

Where θ is the angle of incidence, H is the thickness of the base.

Figure 1. *Simplified schema of a CIGS-based solar cells with one dimensional dimensions.*

In this study, we will neglect the contribution of the emitter by focusing only on the bottom-up contribution.

Under the effect of frequency-modulated monochromatic optical excitation, minority charge (electrons) carriers are generated in the absorbing layer of the solar cells. The continuity equation of the minority carriers in the x-axis base in frequency dynamic regime is of the form [3, 4]:

$$D_\omega \cdot \frac{\partial^2 \delta(x,\theta,t)}{\partial x^2} - \frac{\delta(x,\theta,t)}{\tau} = -G(x,\theta,t) + \frac{\partial \delta(x,\theta,t)}{\partial t} \quad (1)$$

With D_ω the complex diffusion coefficient of minority carriers; $\delta(x,\theta,t)$ the density of minority carriers; $G(x,\theta,t)$ the generation rate of minority carriers [5, 6] and τ the average life of minority carriers.

The density and generation rate of minority carriers can be set respectively in the form [7, 8]:

$$\delta(x,\theta,t) = \delta(x,\theta) e^{(-i\omega t)} \quad (2)$$

$$G(x,\theta,t) = g(x,\theta) e^{(-i\omega t)} \quad (3)$$

Where $\delta(x,\theta)$ and $g(x,\theta)$ are the spatial component and $e^{(-i\omega t)}$ is the temporal component.

For illumination from the front face of the solar cell and depending on the angle of incidence, the spatial component of the generation rate is:

$$g(x,\theta) = \alpha(\lambda)\Phi(\lambda)(1 - R(\lambda)) cos\theta e^{-\alpha(\lambda)x} \quad (4)$$

Where $\alpha(\lambda)$ is the absorption coefficient at the wavelength λ; R(λ) is the reflection coefficient of the material, $\Phi(\lambda)$ the incident photon flux, and θ the incidence angle.

By replacing equations (2), (3) and (4) in equation (1) we get:

$$\frac{\partial^2 \delta(x,\theta)}{\partial x^2} - \frac{\delta(x,\theta)}{L_\omega^2} + \frac{g(x,\theta)}{D_\omega} = 0 \quad (5)$$

with

$$L_\omega = L_0 \sqrt{\frac{(1-i\omega\tau)}{1+(\omega\tau)^2}} \quad (6)$$

L_0: intrinsic diffusion length.

L_ω: the complex diffusion length.

The general solution of the preceding equation (5) is given by the relation (7).

$$\delta(x,\theta) = A cosh\left(\frac{x}{L_\omega}\right) + B sinh\left(\frac{x}{L_\omega}\right) - \frac{\alpha(\lambda)\Phi(\lambda)(1-R(\lambda)).L_\omega^2.cos\theta}{D_\omega.(\alpha^2(\lambda)L_\omega^2 - 1)} e^{-\alpha(\lambda)x} \quad (7)$$

The constants A and B are determined from the following boundary conditions [9]:

i. At junction x=0:

$$\left.\frac{\partial \delta(x,\theta)}{\partial x}\right|_{x=0} = \frac{SF}{D_\omega} \delta(0,\theta) \quad (8)$$

ii. On the rear face of the base (x=H):

$$\left.\frac{\partial \delta(x,\theta)}{\partial x}\right|_{x=H} = -\frac{SB}{D_\omega} \delta(H,\theta) \quad (9)$$

SF and SB denote the recombination speeds of the minority load carriers at the junction and rear face of the base respectively.

The expression of minority carriers' density is expressed as a function of the CIGS absorption coefficient. This coefficient depends on gallium doping and is given by:

$$\alpha(\lambda, X) = A\sqrt{(\frac{hc}{\lambda} - E_g(X))} \quad (10)$$

with A $(cm^{-1}eV^{-1/2})$ a constant [10].

Beyond the expressions of minority carriers' density, photocurrent density and photovoltage are determined according to the angle of incidence of gallium doping rate, frequency and wavelength.

It should be noted that the characteristic photocurrent density -photovoltage of a cell is the curve that reflects the evolution of the photocurrent density that flows through the cell as a function of the photovoltage across its terminals. The exploitation of this characteristic (J_{ph}-V_{ph}) [11] allows us to determine the operating points of the cell. This characteristic will be studied under the effect of the angle of incidence and the doping level with gallium.

Furthermore, the photocurrent-photovoltage density characteristic exhibits an almost vertical plateau where the photovoltage varies little with the photocurrent density. This operating condition of the solar cell corresponds to a voltage source that is equal to the open-circuit photovoltage. This indicates the presence of losses in the solar cell represented by a series resistance R_S. The latter represents the overall resistivity of the material and the metal-grid contacts and is mounted in series with the voltage source in the equivalent circuit.

In Figure 2, the equivalent electrical circuit of the solar cell operating in an open circuit condition is represented [12].

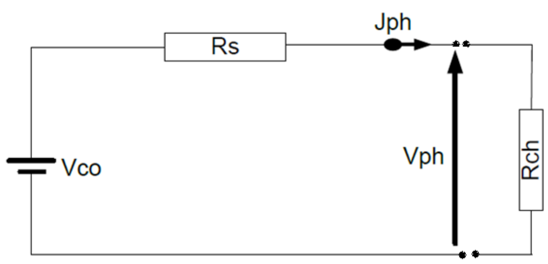

Figure 2. *Equivalent electrical circuit of the solar cell operating in open circuit.*

V_{co}: open-circuit photovoltage; R_S: series resistance; J_{ph}: photo current density; V_{ph}: photovoltage; R_{ch}: load resistance.

By applying the law of meshes, we obtain the following relationship:

$$V_{ph}(SF) = V_{CO} - R_S.J_{ph}(SF) \quad (11)$$

From this equation (11), we obtain:

$$R_S = \frac{V_{CO} - V_{ph}(SF)}{J_{ph}(SF)} \quad (12)$$

$V \rightarrow V_{CO}$
$SF \rightarrow 0$

Furthermore, the characteristic photocurrent-photovoltage density also has a horizontal part that corresponds to a short-circuit photocurrent density zone where the photocurrent density is independent of the variation in photovoltage. This part can be represented by a current generator that delivers a constant electric current regardless of the value of the photovoltage, thus the existence of a leakage current. These effects are represented by an internal load in the photodetector called leakage resistance or shunt resistance.

In figure 3, we represent the equivalent electrical circuit of the solar cell operating in a short-circuit situation. [13].

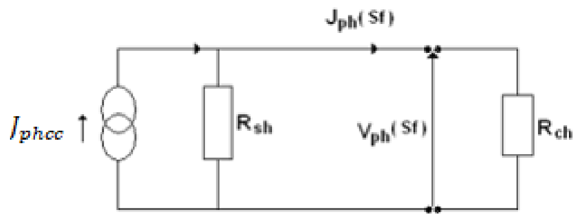

Figure 3. *Equivalent electrical circuit of the solar cell operating in short-circuit conditions.*

J_{phcc}: short-circuit photocurrent density; R_{sh}: shunt resistance; J_{ph}: photo current density; V_{ph}: photovoltage; R_{ch}: load resistance.

The law at the mesh applied to this circuit allows us to write:

$$V_{ph} = R_{sh}(J_{phcc} - J_{ph}) \quad (13)$$

From equation (13) we obtain the following shunt resistance:

$$R_{sh} = \frac{V_{ph}}{J_{phcc} - J_{ph}} \quad (14)$$

$J_{ph} \rightarrow J_{phcc}$
$SF > 10^5 cm.s^{-1}$

These series and shunt resistances will thus be studied under the effects of the angle of incidence of the incident radiation and the gallium doping rate.

3. Results and Discussions

3.1. The Profiles of the Characteristic Photocurrent - Photovoltage (J_{ph}-V_{ph})

Figures 4 and 5 illustrate the characteristic profiles (J_{ph}-V_{ph})

of the photovoltaic cell for each operating point characterized by the recombination speed SF at the junction.

3.1.1. Effect of the Angle of Incidence on the Characteristic (J_{ph}-V_{ph})

Figure 4 presents the characteristic (J_{ph}-V_{ph}) for different values of the angle of incidence of the incident radiation.

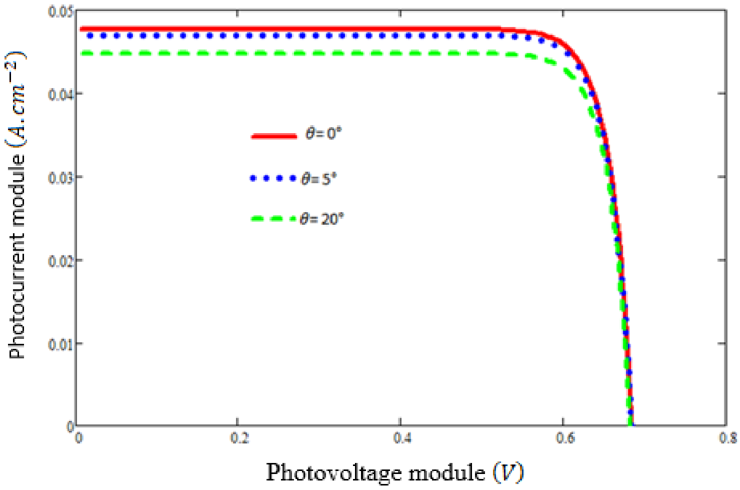

Figure 4. *Characteristic photocurrent density -photovoltage for different values of the angle of incidence.*

$SB = 3.10^3\ cm/s;\ \omega =\ 10^3 rad.s^{-1};$
$\lambda = 0{,}6\ \mu m;\ X = 0{,}3$

In Figure 4, we distinguish two main parts. The first is where the photocurrent density is constant: this part corresponds to the functioning of the photovoltaic cell in a short-circuit situation. The second part where the photocurrent decreases from its short-circuit value to very low values corresponds to the functioning of the photovoltaic cell in an open-circuit situation.

A decrease in short-circuit photocurrent is observed with an increase in the angle of incidence. At the same time, the operating point in open circuit conditions is hardly affected. Thus, the angle of incidence will primarily change the operating point of the photodetaic in short-circuit.

3.1.2. Effect of Gallium Doping Rate on the Characteristic (J_{ph}-V_{ph})

In Figure 5, the effects of the doping rate of Gallium are highlighted on the characteristic. (J_{ph}-V_{ph}).

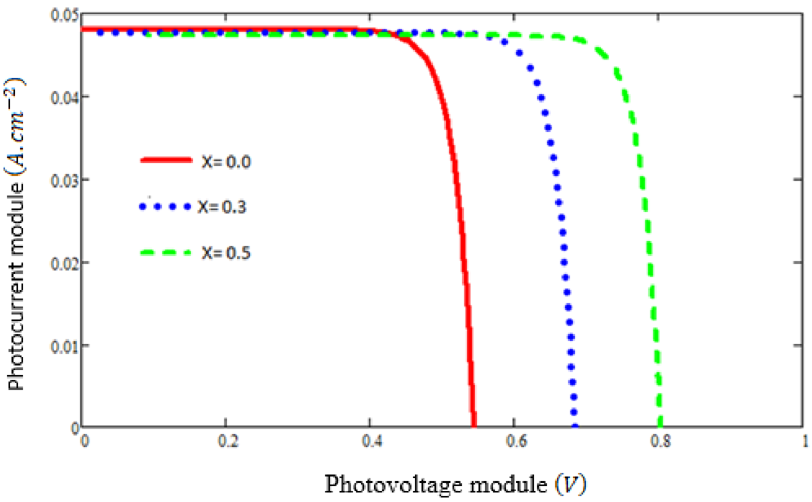

Figure 5. *Characteristic photocurrent density -photovoltage for different gallium doping levels.*

$SB = 3.10^3 \frac{cm}{s}$; $\omega = 10^3 rad.s^{-1}$;
$\lambda = 0{,}6\ \mu m$; $\theta = 0{,}0°$

The observation of the characteristic (J_{ph}-V_{ph}), shows an increase in the open-circuit photovoltage with the doping rate of Gallium. Unlike the effects of the angle of incidence, the Gallium doping rate primarily affects the open-circuit operating point. Thus, we will subsequently study the influence of the angle of incidence and then the Gallium doping rate on the series and shunt resistances.

3.2. Results of Studies on Series Resistance

3.2.1. Effect of the Angle of Incidence on Series Resistance

Figure 6 shows the variation of series resistance as a function of recombination speed at the junction for different values of the angle of incidence.

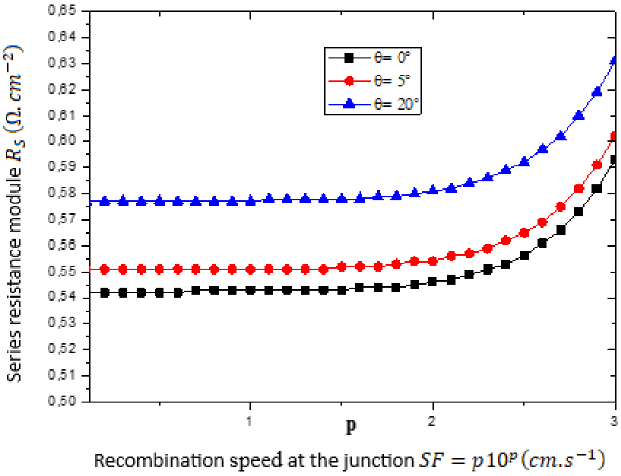

Figure 6. *Module of the series resistance as a function of the recombination speed at the junction for different values of the angle of incidence.*

$SB = 3.10^3 \frac{cm}{s}$; $\omega = 10^3 rad.s^{-1}$;
$\lambda = 0{,}6\ \mu m$; $X = 0{,}3$

We observe an increase in the series resistance with the recombination speed at the junction. Indeed, the increase in the recombination speed at the junction in an open circuit increases charge accumulation by generating V_{CO}. This leads to an increase in volume and surface recombinations, and therefore an increase in the series resistance. We notice that the magnitude of the series resistance increases with the increase in the angle of incidence. Indeed, even though the increase in the angle of incidence is accompanied by a low generation of charge carriers, their accumulation in an open circuit promotes losses at the interface, hence an increase in the magnitude of the series resistance.

3.2.2. Effect of the Doping Rate of Gallium on Series Resistance

In Figure 7, we present the profile of the modulus of the series resistance as a function of the recombination speed at the junction for different gallium doping levels.

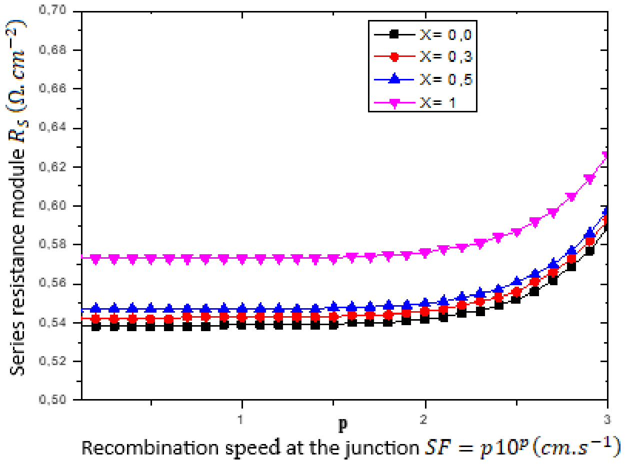

Figure 7. *Series resistance module as a function of the recombination speed at the junction for different doping rates of gallium.*

$SB = 3.10^3 \frac{cm}{s}$; $\omega = 10^3 rad.s^{-1}$;
$\lambda = 0{,}6\ \mu m$; $\theta = 0{,}0°$

Figure 7 shows the same curve profile as figure 6. We observe an increase in series resistance with the increase in gallium doping rate. This increase mainly arises from the effects of the gallium doping rate on the CdS/CIGS interface. Moreover, a preferential increase in gallium concentration near the Mo back contact may well reduce the series resistance [14].

3.3. Results of Shunt Resistance Studies

3.3.1. Effect of the Angle of Incidence on Shunt Resistance

The following figure 8 shows the variation of the shunt resistance module as a function of the recombination velocity at the junction for different values of the angle of incidence.

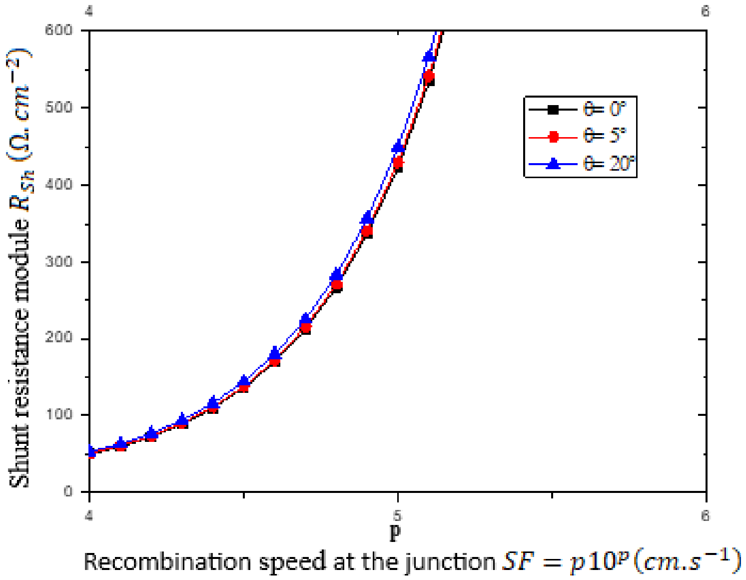

Figure 8. *Shunt resistance module as a function of the recombination velocity at the junction for different values of the angle of incidence.*

$SB = 3.10^3\,\frac{cm}{s}$; $\omega = 10^3 rad.s^{-1}$;
$\lambda = 0{,}6\,\mu m$; $X = 0{,}3$

For a given wavelength, the shunt resistance increases exponentially with the recombination speed at the SF junction ($SF > 5.10^5 cm/s$). This results in a strong recombination of carriers at the junction. We also observe that the magnitude of the shunt resistance slightly increases with the increase of the angle of incidence. The attenuation of light intensity with the increase of the angle of incidence promotes recombinations between intermediate bands, thus increasing leakage currents.

3.3.2. Effect of the Doping Rate of Gallium on Shunt Resistance

In Figure 9, we represent the profile of the shunt resistance module as a function of the recombination speed at the junction for different values of gallium doping levels.

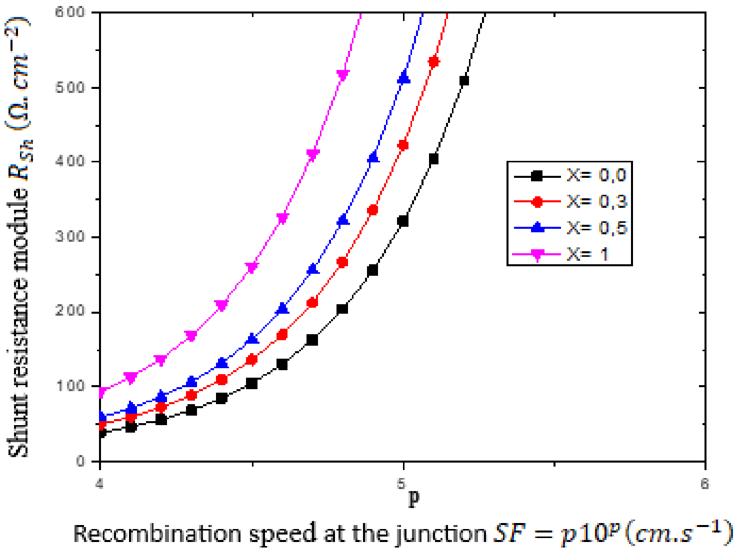

Figure 9. *Shunt resistance module as a function of recombination speed at the junction for different gallium doping rates.*

$SB = 3.10^3\,\frac{cm}{s}$; $\omega = 10^3 rad.s^{-1}$;
$\lambda = 0{,}6\,\mu m$; $\theta = 0{,}0°$

In this figure 9, the variation of the shunt resistance as a function of the recombination rate at the junction for different values of the gallium doping level is illustrated. It is observed that the shunt resistance increases exponentially with high recombination rates at the SF junction (photocell under short-circuit conditions). Furthermore, the increase in gallium doping level also raises the shunt resistance. It should be noted that the increase in gallium doping level is accompanied by an increase in the depletion zone, which could lead to higher leakage and thus an increase in shunt resistance.

4. Conclusion

This article highlights the effect of gallium doping rate and the angle of incidence on the photocurrent-photovoltage characteristic as well as the series and shunt resistances. A more significant effect of the angle of incidence on the short-circuit operating point of the solar cell is observed, as well as a similarly significant effect of the gallium doping rate on the open-circuit operating point of the cell. Furthermore, both the gallium doping rate and the angle of incidence increase the series and shunt resistances.

Author Contributions

Gerome Sambou: Conceptualization, Data curation, Formal Analysis, Funding acquisition, Investigation, Methodology, Project administration, Resources, Software, Validation, Visualization, Writing – original draft, Writing – review & editing,

Ibrahima Wade: Formal Analysis, Funding acquisition, Methodology, Resources, Validation

Khamissa Diallo: Formal Analysis, Resources

Djimba Niane: Formal Analysis, Methodology, Resources

Moustapha Dieng: Methodology, Supervision, Validation, Writing – review & editing

Conflicts of Interest

The authors declare no conflicts of interest.

Appendix

Table A1. *Symbol and Definition.*

$\delta(x,\theta,t)$	density of minority carriers	(cm^{-3})
J_{ph}	Photocurrent density module	($A.cm^{-2}$)
J_{phcc}	short-circuit photocurrent density	($A.cm^{-2}$)
ω	Angular frequency	($rad.s^{-1}$)
λ	Wavelength	(μm)
Rs	Series resistance	($\Omega.cm^{-2}$)
Rsh	Shunt resistance	($\Omega.cm^{-2}$)
V_{ph}	Photovoltage Module	(V)
V_{co}	Open-circuit photovoltage	(V)
SF	Recombination Speed at the junction	($cm\ s^{-1}$)
SB	Recombination speed at the rear face	($cm\ s^{-1}$)
X	Gallium doping rate	
P	Solar cell power	($W.cm^{-2}$)
FF	Form factor	(%)
η	Cell efficiency	(%)

References

[1] Michael Powalla, Stefan Paetel, Dimitrios Hariskos al. «Advances in Cost-Efficient Thin-Film Photovoltaics Based on Cu(In, Ga)Se_2» *Engineering*, Volume 3, Issue 4(2017), pages 445–451. https://doi.org/10.1016/J.ENG.2017.04.015

[2] Seung Hoon Lee, Hae Seok Lee, Donghwan Kim, Yoonmook Kang "The Diagnosis of Shunt Defects in CIGS Modules Using Lock-In Thermography: An Empirical Comparative Study" MDPI *Energies*, vol 16, no 21, (2023).

[3] N. Honma and C. Munakata, «Sample thickness dependence of minority carrier lifetimes measured using an ac photovoltaic method», Japan. J. Appl. Phys. 26, (1987) 2033-6. https://doi.org/10.1143/JJAP.26.2033

[4] A. Dieng, I. Zerbo, M. Wade, A. S. Maiga et G. Sisoko, «Three-dimensional study of a polycrystalline silicon solar cell: the influence of the applied magnetic field on the elctrical parameters», Semicond. Sci. Technol. 26, (2011) pp: 5023-5032.

[5] J. N. Hollenhorst et G. Hasnain, «Frequency dependent whole diffusion in InGaAs double heterostructure» Appl. Phys. Lett, 65(15): (1995) 2203-2205.

[6] F. Ahmed et S. Garg, «simultaneous determination of diffusion length, lifetime and diffusion constant of minority carrier using a modulated beam» International Atomic Energy Agency. International centre for theorical physics. Internal report IC/86/129, 1987.

[7] J. Dugas, «3D modelling of a reverse cell made with improved multicrystalline silicon wafers». Solar Energy Materials and Solar Cells Volume 32. Issue 1, (January 1994). Pages 71-88. https://doi.org/10.1016/0927-0248(94)90257-7

[8] T. Flohr et R. Helbig, «Determination of minority-carrier lifetime and surface recombination velocity by Optical-Beam-Iduced-Current measurements at different light wavelengths» J. Appl. Phys. Vol. 66(7), (1989) pp 3060-3065. https://doi.org/10.1063/1.344161

[9] Sissoko, G., Museruka, C., Corréa, A., Gaye, I. and Ndiaye, A. L. (1996) Light Spectral Effect on Recombination Parameters of Silicon Solar Cell. World Renewable Energy Congress, Part III, 1487-1490.

[10] Morales-Acevedo «Effective absorption coefficient for graded band-gap semiconductors and the expected photocurrent density in solar cells». Solar Energy Materials & Solar Cells 93(2009) 41-44. https://doi.org/10.1016/j.solmat.2008.02.015

[11] S. Mbodji, B. Mbow, F. I. Barro et G. Sissoko, «A 3D model for thickness diffusion capacitance of emitter-base junction determination in a bifacial polycrystalline solar cell under real operating condition», Turk. J. Phys. 35 281-291, 2011.

[12] El-Adawi M. K. and Al-Nuaim I. A., “A method to determine the solar cell series resistance from a single I-V characteristic curve considering its shunt resistance – new approach,” *Vacuum, 64, pp. 33- 36, 2002*. https://doi.org/10.1016/S0042-207X(01)00370-0

[13] I. ZERBO, F. I. BARRO, B. MBOW, A. DIAO, F. ZOUGMORE, G. SISSOKO “Theoretical Study of Bifacial Silicon Solar Cell Under Frequency Modulated White Light: Determination of Recombination Parameters”. Proceedings of the 19th European Photovoltaic Solar Energy Conference (2004), Poster 1AV.2.56, Paris, FRANCE.

[14] Johnathan Charles Armstrong, Jingbiao Cui «Optimization of solution-processed Cu(In, Ga)S_2 by tuning series and shunt resistance» J. Mater. Res., Vol. 29, No. 11, Jun 14, 2014.